

# Atomic steps with tuning-fork-based noncontact atomic force microscopy

W. H. J. Rensen<sup>a)</sup> and N. F. van Hulst

*Applied Optics Group, University of Twente, P.O. Box 217, 7500AE Enschede, The Netherlands*

A. G. T. Ruiter and P. E. West

*ThermoMicroscopes, RD&E Department, 1171 Borregas Avenue, Sunnyvale, California 94089*

(Received 27 April 1999; accepted for publication 19 July 1999)

Tuning forks as tip-sample distance detectors are a promising and versatile alternative to conventional cantilevers with optical beam deflection in noncontact atomic force microscopy (AFM). Both theory and experiments are presented to make a comparison between conventional and tuning-fork-based AFM. Measurements made on a Si(111) sample show that both techniques are capable of detecting monatomic steps. The measured step height of 0.33 nm is in agreement with the accepted value of 0.314 nm. According to a simple model, interaction forces of 30 pN are obtained for the tuning-fork-based setup, indicating that, at the proper experimental conditions, the sensitivity of such an instrument is competitive to conventional lever-based AFM. © 1999 American Institute of Physics. [S0003-6951(99)05337-1]

Atomic force microscopy (AFM) is increasingly becoming a tool for high-tech industrial applications. Routine metrology on wafers or masks, magnetic force microscopy on data storage media are just a few of numerous applications. To prevent tip or sample damage, noncontact mode operation is preferred for these applications. In conventional AFM, the cantilever with optical beam deflection (light-lever) technique has several disadvantages. First of all, it introduces noise in the setup due to thermal mode hopping of the laser and drift caused by heat dissipation of the laser diode.<sup>1</sup> Second, the alignment of the laser beam on the cantilever and the position sensitive photo detector is an elaborate process. Third, the need of a laser diode, an adjustable mirror, and a photo detector prevent the miniaturization of the scanning head. These disadvantages suggest the use of a nonoptical feedback method.

In near-field scanning optical microscopy (NSOM), the use of a nonoptical feedback has been apparent for a longer time. At this moment the tuning-fork-based height feedback is widespread.<sup>2,3</sup> The advantages are clear. The tuning fork is a cheap, small height detector. No optical alignment is needed and a simple and compact instrument can be designed around it. In NSOM, the tuning fork is usually operated in a way that the probe is oscillated parallel to the sample surface: shear force microscopy. Another option is to oscillate the probe perpendicular to the surface, as in light-lever based noncontact AFM. This way of operation is better understood and believed to be more reliable.<sup>4-7</sup> As the tuning fork is an appealing nonoptical height detection sensor, several tuning-fork-based setups have been implemented.<sup>8-11</sup>

In this study, the sensitivity of a tuning-fork-based system is explored and compared to a light-lever based AFM in noncontact mode. A simple model is presented that can be used for both techniques. After that, the results of measurements on a Si(111) sample are presented and discussed using the presented model.

In a first approximation tuning forks and cantilevers can

be considered as damped harmonic oscillators, with spring constant  $k$ , damping constant  $\gamma$ , and effective mass  $m$ . In the present setup the oscillator is excited using a displacement  $x_d = |x_d| \exp(i\omega t)$  with constant driving amplitude  $|x_d|$  and at constant frequency  $\omega$ . Both the resulting oscillation amplitude  $|x|$  and the phase with respect to the drive  $\varphi$  of the displacement  $x = |x| \exp(i\omega t + \varphi)$  can be monitored as the height signal. The equation of motion for such a system is:  $\gamma(\dot{x}_d - \dot{x}) + k(x_d - x) = m\ddot{x}$ , where the dot indicates a time derivative. Having only harmonic time dependence, this leads to the following solution:

$$\frac{x}{x_d} = \frac{i\omega(\gamma/m) + (k/m)}{(k/m) + i\omega(\gamma/m) - \omega^2}. \quad (1)$$

This solution has complex frequency dependence, so both an amplitude ratio and a phase shift between  $x$  and  $x_d$  can be found. For systems with small damping ( $\gamma/m \ll \omega_{\text{res}}$ ), the resonance frequency, the frequency where  $|x/x_d|$  is maximal, does not depend on the damping constant:  $\omega_{\text{res}}^2 = k/m$  and the  $Q$  factor is in good approximation equal to the amplification of the driving amplitude at resonance.

$$\left| \frac{x}{x_d} \right|_{\text{res}} \approx \frac{m\omega_{\text{res}}}{\gamma} = \frac{\sqrt{km}}{\gamma} \approx Q. \quad (2)$$

The resonance curve of a harmonic oscillator is given in Fig. 1. Figure 1(a) is the amplitude-frequency plot and Fig. 1(b) is the phase-frequency plot. The frequency scale is normalized so that the resonance frequency is at 1. The amplification scale is normalized to the excitation amplitude.

The tip-sample interaction is modeled as an extra damping  $\Delta\gamma$  and an extra spring  $\Delta k$  with  $\Delta\gamma \ll \gamma$  and  $\Delta k \ll k$ . This is a simple alternative to a Hertzian contact model<sup>10</sup> and an expansion to the viscous damping model.<sup>2</sup>

If the interaction results in a small extra damping, the total damping of the system will change to  $\gamma + \Delta\gamma$ . The effect of increased damping is indicated in Fig. 1. The resonance frequency of the resonator hardly changes and the phase lag of the resonator stays at  $\pi/2$ . The  $Q$  factor and thus

<sup>a)</sup>Electronic mail: w.h.j.rensen@tn.utwente.nl

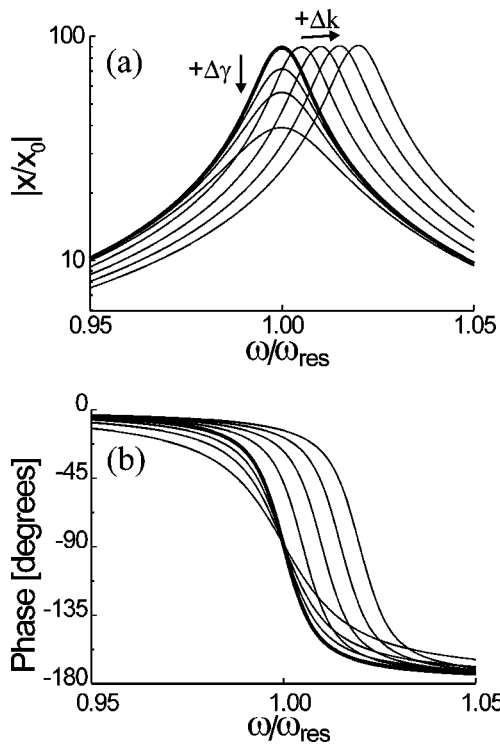


FIG. 1. Bode plots of the harmonic oscillator model. Both the influence of an increased spring constant  $\Delta k$  and the influence of increased damping  $\Delta \gamma$  on the undisturbed harmonic oscillator are shown.

the amplitude of the oscillator drops with  $\Delta x$ . In this case, the amplitude of the resonator is the only suitable signal to monitor.

The tip-sample distance is usually regulated to achieve a constant amplitude-damping  $\Delta x$ . The interaction force can be calculated by adding a virtual damping element  $\Delta \gamma$  that corresponds with  $\Delta \gamma$ . The interaction force is equal to the force applied to this virtual damping element

$$F_{\text{interaction}} = \frac{kx_{\text{res}}}{Q} \frac{\Delta x}{x_{\text{res}}}, \tag{3}$$

where  $x_{\text{res}}$  is the amplitude of the resonator at resonance. The interaction as a small extra spring is investigated in a similar way. The total spring constant in the system will increase to  $k + \Delta k$ . The effect of an increasing spring constant is also indicated in Fig. 1. The resonance frequency and the  $Q$  factor of the resonator increase. As the driving frequency is still at the original value, the phase lag and the amplitude of the resonator change. Being at a maximum slope, the phase lag will change most, so for a change in spring constant, it is best to monitor the phase signal.

Again it is possible to calculate the interaction force. The tip-sample distance is regulated to achieve a constant preset phase shift  $\Delta \varphi$ . After calculating the corresponding extra spring constant, it is easy to calculate the force applied to this extra spring in a first order approximation.

$$F_{\text{interaction}} = \frac{kx_{\text{res}}}{Q} \Delta \varphi. \tag{4}$$

The best signal to monitor, amplitude or phase of a resona-



FIG. 2. Tuning fork with Si cantilever attached to it.

tor, depends on how the interaction is best described, causing a change in the effective spring constant or in the effective damping constant.

In the experiment performed to compare the two techniques, the light-lever based AFM is operated with a standard Si-cantilever probe reflecting the light from a laser diode. The reflected light is detected by a position sensitive photodiode. The signal from the photodiode is amplified by a transimpedance amplifier and then demodulated and further processed by the electronics of the instrument.<sup>12</sup> The amplitude of the cantilever deflection was used for tip-sample distance control.

For the tuning-fork-based setup, the same type of Si cantilever is glued on top of a tuning fork, as shown in Fig. 2. The free length of the cantilever is made short enough to make it rigid at the resonance frequency of the tuning fork. A transimpedance amplifier amplified the piezoelectric signal from the tuning fork and a lock-in amplifier extracted the amplitude or phase. Ruiter *et al.*<sup>13</sup> have found that during approach towards the sample with a tuning-fork-based system, mostly a shift in resonance frequency occurs, corresponding to an increase in spring constant. This and the relatively high  $Q$  factor of the tuning fork, the choice for this experiment is to use the phase signal for the tuning-fork-based setup.

Except for the probes and the detection electronics, the same instrument<sup>12</sup> was used for the comparison. Several parameters and operating conditions for the two different techniques are given in Table I.

The used sample is a Si(111) sample provided by the National Institute of Standards and Technology (NIST).<sup>14</sup> It is prepared in a way that stable monatomic steps with a step height of 0.314 nm<sup>15</sup> are present in ambient conditions. In air there will be an oxide layer, but this layer has a constant thickness and does not affect the step heights in the sample.

Figure 3 shows the topography measured with tuning-fork-based AFM and Fig. 4 shows the topography of the same sample, however measured with light-lever based AFM. No image processing is done, except for subtracting a parabola at each scan line (second order line leveling) to compensate for sample tilt, angular scanner movement, and

TABLE I. Selected parameters on light-lever and tuning-fork-based AFM.

	Light-lever	Tuning-fork
$k$	48 N/m	45 kN/m
$Q$	360	2600
$\omega_{\text{res}}$	143 kHz	97.7 kHz
Operating conditions		
$x_{\text{res}}$	5.4 nm	0.1 nm
$\Delta x$	2.7 nm	
$\Delta \varphi$		1°
$F_{\text{int}}$	360 pN	30 pN

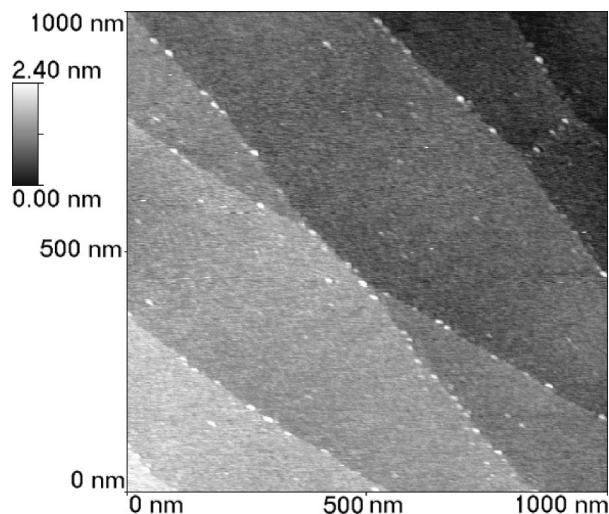


FIG. 3. Monatomic steps on Si(111) measured with a tuning fork based setup.  $1\ \mu\text{m}\times 1\ \mu\text{m}$  scan area,  $500\times 500$  pixels, line frequency 0.25 Hz. The measured step height is 0.33 nm with a rms noise over the area of 0.14 nm. A double step height is measured at step crossings. Small particles are clearly visible suggesting small interaction forces. The calculated interaction force is 30 pN.

drift due to temperature fluctuations during scanning. The observed step height is 0.33 nm for both techniques with an rms noise over the area of 0.09 nm for the light-lever based AFM and 0.14 nm for the tuning-fork-based AFM.

In the comparison, two different signals have been used for tip-sample distance control. The amplitude of the cantilever for the light-lever based AFM and the phase of the tuning fork in the tuning-fork-based AFM. To make the comparison still fair, the operation conditions as given in Table I, were chosen so that the rms noise over the area was approximately the same for both measurements.

In both images, the monatomic steps are clearly visible. The step height is twice the step height of one single step at places where two steps coincide, an indication that these are

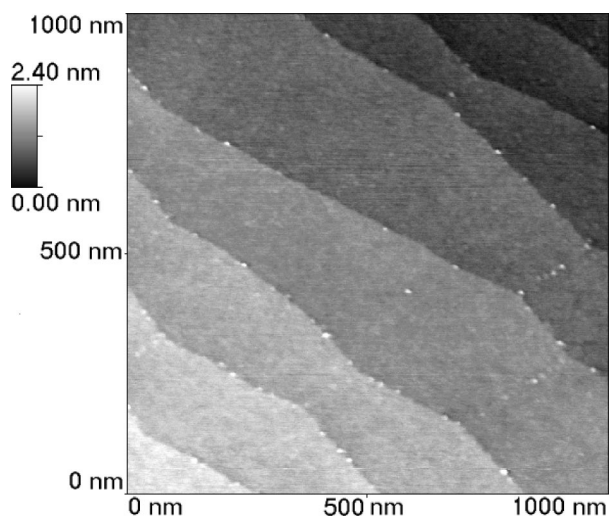


FIG. 4. Monatomic steps on Si(111) measured with a light-lever based setup.  $1\ \mu\text{m}\times 1\ \mu\text{m}$  scan area,  $500\times 500$  pixels, line frequency 1 Hz. The measured step height is 0.33 nm with a rms noise over the area of 0.09 nm. Only a few small particles are visible compared to Fig. 3, suggesting larger interaction forces for light-lever based AFM. The calculated interaction force is 360 pN.

indeed monatomic steps. Also the measured height of the steps is in agreement with the expected value of 0.314 nm for both techniques. The interaction forces calculated with the harmonic oscillator model indicate a lower interaction force of 30 pN for the tuning-fork-based setup compared to the interaction force of 360 pN obtained with the light-lever based AFM. The results with the tuning-fork-based AFM are close to the thermal limit of 5.3 pN at room temperature.<sup>2</sup> The light-lever based AFM is still far from its thermal limit of 1.3 pN. More small particles are visible in the measurement with the tuning-fork-based AFM. A possible explanation is that the light-lever based AFM swept the dust away. This would confirm that the forces applied to the sample by the tuning-fork-based setup are indeed lower.

The measurements of monatomic steps on a Si(111) sample demonstrate the sensitivity of the tuning fork as a height detector. In the experiments performed, the sensitivity is one order of magnitude better than noncontact AFM cantilevers. Choosing smaller amplitude damping as the feedback set point will lower the interaction forces of the light-lever based AFM ultimately down to the thermal limit. Cleveland *et al.* have shown that the thermal limit can indeed be the ultimate limit for AFM.<sup>16</sup> Increasing the  $Q$  factor of the tuning fork can lower the interaction forces and the thermal limit for force detection of the tuning-fork-based AFM. With quartz tuning forks,  $Q$  factors in the order of  $10^4$ – $10^5$  can be obtained. In the present setup that uses a constant driving frequency, this will prevent fast scanning, but implementing a self-oscillating circuit and using the resonance frequency as the tip-sample distance signal, will circumvent this problem.

As tuning forks do not need any optics for height detection, probe replacement is easy and tolerant. It further allows a more compact scan head and even multiple scan heads on one sample. The high sensitivity and the lack of optics can make a tuning-fork-based setup the preferred choice in industrial applications, where simple operation, quick probe replacement, and throughput are important.

<sup>1</sup>Z. Dai, M. Yoo, and A. de Lozanne, *J. Vac. Sci. Technol. B* **14**, 1591 (1996).

<sup>2</sup>K. Karrai and R. D. Grober, *Appl. Phys. Lett.* **66**, 1842 (1995).

<sup>3</sup>A. G. T. Ruiter, J. A. Veerman, K. O. van der Werf, and N. F. van Hulst, *Appl. Phys. Lett.* **71**, 28 (1997).

<sup>4</sup>A. G. T. Ruiter, Ph.D. thesis, University of Twente, 1997, p. 34.

<sup>5</sup>M. J. Gregor, P. G. Blome, and J. Schöfer, *Appl. Phys. Lett.* **68**, 307 (1996).

<sup>6</sup>H. J. Ho, *Proc. SPIE* **3512**, 40 (1998).

<sup>7</sup>N. A. Burnham, R. J. Colton, and H. M. Pollock, *J. Vac. Sci. Technol. A* **9**, 2548 (1991).

<sup>8</sup>Th. Murfield, U. C. Fischer, H. Fuchs, R. Volk, A. Michels, F. Meinen, and E. Beckman, *J. Vac. Sci. Technol. B* **14**, 877 (1996).

<sup>9</sup>H. Edwards, L. Taylor, W. Duncan, and A. J. Melmed, *J. Appl. Phys.* **82**, 980 (1997).

<sup>10</sup>F. J. Giessibl, *Appl. Phys. Lett.* **73**, 3956 (1998).

<sup>11</sup>D. P. Tsai and Y. Y. Lu, *Appl. Phys. Lett.* **73**, 2724 (1998).

<sup>12</sup>The instrument used as a basis for these experiments was a Discoverer manufactured by ThermoMicroscopes, 1171 Borregas Avenue, Sunnyvale, CA 94089.

<sup>13</sup>A. G. T. Ruiter, K. O. van der Werf, J. A. Veerman, M. F. Garcia-Parajo, W. H. J. Rensen, and N. F. van Hulst, *Ultramicroscopy* **71**, 149 (1998).

<sup>14</sup>NIST, 100 Bureau Drive, Gaithersburg, MD 20899.

<sup>15</sup>V. Tsai, X.-S. Wang, E. D. Williams, J. Schneir, and R. Dixon, *Appl. Phys. Lett.* **71**, 1495 (1997).

<sup>16</sup>J. P. Cleveland, T. E. Schäffer, and P. K. Hansma, *Phys. Rev. B* **52**, 8692 (1995).